ANTICANCER RESEARCH *41*: 1803-1810 (2021)
doi:10.21873/anticanres.14946

Sinusoidal Obstruction Syndrome Promotes Liver Metastatic Seeding of Colorectal Cancer Cells in a Rat Model

HIROTO NISHINO[1], MASAYUKI OKUNO[1,2], SATORU SEO[1], REI TODA[1], KENJI YOSHINO[1], YOSUKE KASAI[1], MOTOHIKO SATOH[1], KEIKO IWAISAKO[3], KOJIRO TAURA[1] and ETSURO HATANO[1,2]

[1]*Department of Surgery, Graduate School of Medicine, Kyoto University, Kyoto, Japan;*
[2]*Department of Gastroenterological Surgery, Hyogo College of Medicine, Nishinomiya, Japan;*
[3]*Department of Medical Life Systems, Faculty of Life and Medical Sciences, Doshisha University, Kyotanabe, Japan*

Abstract. *Background/Aim: Sinusoidal obstruction syndrome (SOS) after neoadjuvant chemotherapy with oxaliplatin for colorectal liver metastases (CRLM) has been reported to lead to early recurrence. This study investigated the effects of SOS on the development of CRLM in a rat model. Materials and Methods: RCN-H4 cells were injected into the spleen or liver of ten monocrotaline-treated (SOS group) and ten untreated (control group) rats. The number and size of liver tumors were compared between the groups. Results: The number of liver tumors in the splenic RCN-H4 injection model was significantly higher in the SOS group than in the control group (332±213 vs. 16±5, p=0.029); however, the largest tumor diameter in the hepatic model was similar between groups (6.2±1.8 vs. 6.4±2.4 mm, p=0.87). Conclusion: SOS promotes CRLM development by splenic RCN-H4 cell injection. This might be due to the higher incidence of cancer cell implantation into the liver.*

Approximately 15% of patients with colorectal cancer have synchronous liver metastases, and approximately 30% of them transition to metachronous liver metastases (1). Liver surgery is the only potentially curative treatment for patients with colorectal liver metastases (CRLM) and is associated with long-term survival (2). Recent advances in systemic chemotherapy and multidisciplinary treatment strategies such as two-stage hepatectomy and a liver-first approach have made it possible to transform unresectable CRLM to resectable CRLM, which is called conversion therapy (3-5).

Sinusoidal obstruction syndrome (SOS), characterized by sinusoidal dilatation, central venous endothelial damage, and coagulative necrosis of hepatocytes, is a common drug-induced liver injury caused by chemotherapy regimens using oxaliplatin as treatment for CRLM (6, 7). SOS is often referred to as "blue liver disease", and it impairs the resectability of the liver by decreasing its regenerative capacity and functional reserve (8).

Tamandl *et al.* reported that SOS after neoadjuvant chemotherapy with oxaliplatin was associated with increased postoperative morbidity and resulted in early recurrence and decreased long-term survival in CRLM (9). However, its underlying mechanism remains unclear, and an optimal animal model to investigate the mechanism has not been established to date.

This study aimed to establish an appropriate mimic model of SOS after human oxaliplatin-induced liver injury and clarify whether SOS influences CRLM development in an MCT-induced rat model.

Materials and Methods

We used the most prevalent and common animal model for SOS studies, namely a monocrotaline (MCT)-induced rat model, which has been the basis for diagnostic and treatment studies and has been modified over the past two decades to optimize its use (10-16).

Animals. Five- to six-week-old male Fischer 344 rats (SLC, Shizuoka, Japan) weighing 150-200 g were used. All rat surgical procedures were performed under general anesthesia with isoflurane. All experiments were conducted according to the guidelines for the care and use of laboratory animals of the animal research committee of Kyoto University (approval code: Med Kyo 19186). The animals received humane care according to the National Institutes of Health (Bethesda, MD, USA) Guidelines for the Care and Use of Laboratory Animals.

Correspondence to: Masayuki Okuno, MD, Ph.D., Department of Gastroenterological Surgery, Hyogo College of Medicine, 1-1 Mukogawa-cho, Nishinomiya, Hyogo, 663-8501, Japan. Tel: +81 798456582, e-mail: okunovic@kuhp.kyoto-u.ac.jp and Satoru Seo, MD, Ph.D., Department of Surgery, Graduate School of Medicine, Kyoto University, 54 Kawahara-cho, Shogoin, Sakyo-ku, Kyoto, 606-8507, Japan. Tel: +81 757513234, e-mail: rutosa@kuhp.kyoto-u.ac.jp

Key Words: Colorectal cancer, liver metastasis, sinusoidal obstruction syndrome, cancer microenvironment, monocrotaline.

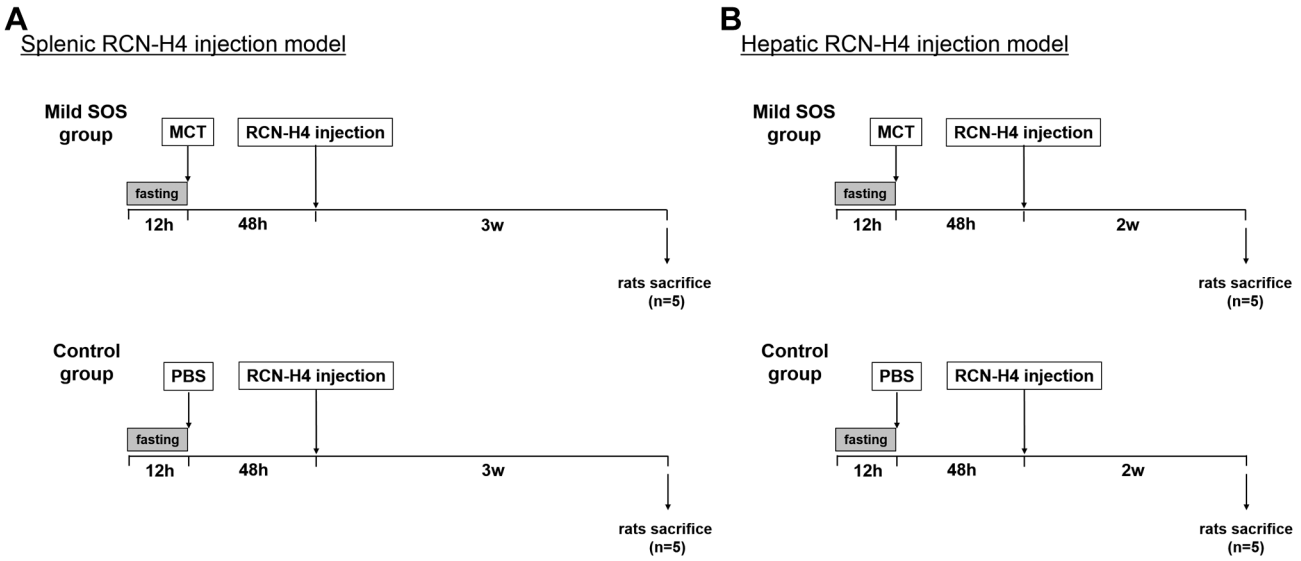

Figure 1. *Experimental protocol for the evaluation of monocrotaline (MCT)-induced mild sinusoidal obstruction syndrome for tumor progression. (A) splenic RCN-H4 injection model, (B) hepatic RCN-H4 injection model. MCT, Monocrotaline; SOS, sinusoidal obstruction syndrome; PBS, phosphate-buffered saline.*

Reagents. MCT was purchased from Sigma Aldrich (St. Louis, MO, USA). MCT solution was prepared at a concentration of 10 mg/ml, as previously reported (17).

Cell line and cell culture. The rat colorectal cancer RCN-H4 cell line (18, 19), derived from liver metastasis of a Fischer 344 rat, was maintained at 37˚C under 5% CO_2 in Roswell Park Memorial Institute 1640 medium (RPMI 1640; Invitrogen, Carlsbad, CA, USA) supplemented with 10% fetal bovine serum (ICN, Aurora, OH, USA), 100 U/ml penicillin G, and 100 μg/ml streptomycin (Meiji Seika, Tokyo, Japan). Cells were passaged every 3-5 days. Cell suspensions were obtained from confluent culture dishes using a trypsin solution, and the cell number was determined using a hemocytometer.

Establishment of liver metastases. Before laparotomy, the entire abdomen was sterilized with a 70% ethanol solution. To establish liver metastases through the portal vein, a 5 mm subcostal incision was made on the left flank through the skin and peritoneum. Rat cancer cells (1.0×10^6 RCN-H4) were suspended in 0.5 ml of phosphate-buffered saline (PBS) into the spleen. Then, the spleen was carefully returned to its anatomical position in the peritoneal cavity, and the abdominal wall and skin were closed.

To establish locally formed liver metastases, a 10 mm incision was made vertically in the midline of the upper abdomen through the skin and peritoneum. Rat cancer cells (1.0×10^6 RCN-H4) were suspended in 0.5 ml of PBS in the left lateral liver lobe. The liver was then carefully returned to its anatomical position in the peritoneal cavity and the abdominal wall and skin were closed.

In both cell line injection routes, the injection procedure itself was confined to a single location within the substance of the organ for more 15 s using a 30-gauge needle. Hemostasis over the puncture site was achieved with slight pressure on the organ with a cotton swab for 5 min (20).

Comparison of SOS severity among high-dose MCT, low-dose MCT, and control groups. Rats were fasted for 12 h before oral MCT administration with free access to water. MCT was administered by gavage, after which the rats could consume food and water ad libitum. To evaluate the degree of SOS, the rats were divided into three groups (n=4 in each group) treated with high-dose MCT group (90 mg/kg), low-dose MCT group (70 mg/kg), or control group (7 ml/kg PBS as vehicle). The rats were sacrificed 48 h after MCT or vehicle administration, and blood and liver tissue samples were collected.

Comparison of tumor progression between the MCT-induced mild SOS group and control group in the splenic injection model. To evaluate the effect of SOS on liver metastatic seeding of colorectal cancer cells, the rats were divided into two groups according to the treatment with 70 mg/kg MCT (mild SOS group) or vehicle (control group; n=5 in each group). In both groups, 48 h after MCT or vehicle administration, RCN-H4 cells were implanted to five rats by splenic injection. All rats were sacrificed after 21 days of monitoring, and the tumors were counted (Figure 1A).

Comparison of tumor progression between the MCT-induced mild SOS group and control group in the liver injection model. To evaluate the effect of SOS on hematogenous metastasis, the rats were divided into a mild SOS group or control group (n=5 in each group). In both groups, 48 h after MCT or vehicle administration, RCN-H4 cells were implanted to five rats by hepatic injection. All rats were sacrificed after 14 days of monitoring, and tumor size of the tumor was measured (Figure 1B).

Comparison of hepatic mRNA expression of genes 48 h after MCT or vehicle administration between the mild SOS and control groups. To evaluate background live damage, hepatic mRNA expression of genes between the mild SOS and control groups (n=4 in each group)

Table I. *The sequence of primers used for reverse transcription and quantitative PCR reactions.*

Gene	Forward primer sequence (5'-3')	Reverse primer sequence (5'-3')
VEGF-A	ATTGAGACCCTGGTGGAC	CCTATGTGCTGGCTTTGG
MMP-9	ACTCGAGCCGACGTCACTGT	GGCCCTCGCCGGTACAGGTA
ICAM-1	CTTTGCCCTGGTCCTCCAAT	TGTCTTCCCCAATGTCGCTC
GAPDH	TCCCTCAAGATTGTCAGCAA	AGATCCACAACGGATACATT

was measured using liver tissues excised 48 h after MCT or vehicle administration.

Serum biochemistry. Serum aspartate aminotransferase (AST), alanine aminotransferase (ALT), and albumin levels were measured 48 h after treatment.

Histopathology. Liver tissue samples were fixed with 4% paraformaldehyde (PFA), embedded in paraffin wax, and cut into 4 mm sections. Histological assessment of SOS was performed using hematoxylin and eosin (H&E) staining.

Immunohistochemistry. Endothelial cells were stained using rat endothelial cell antigen-1 (RECA-1: MCA-970R; AbD Serotec, Oxford, United Kingdom), as previously described (12-16). Tissues were directly embedded in the optimal cutting temperature compound (Sakura, Tokyo, Japan). Sections were cut at 6-mm thickness and fixed with 4% PFA for 10 min at room temperature. Sections were blocked and then incubated with RECA-1 at a 1:500 dilution for 1 h at 4˚C. Subsequently, the sections were incubated with labeled polymer using an EnVision and System HRP kit (Dako, Tokyo, Japan), at room temperature for 1 h. The sections were examined after incubation using the Liquid 3, 3'-diaminobenzidine Substrate-Chromogen System (Dako).

Quantitative real-time polymerase chain reaction. Total RNA was extracted from the liver tissue using TRIzol reagent (Life Technologies, Carlsbad, CA, USA) and the RNeasy Mini Kit with on-column DNA digestion (Qiagen, Valencia, CA, USA). The extracted RNA was reverse transcribed to complementary DNA using the Omniscript RT kit (Qiagen). Quantitative real-time polymerase chain reaction was performed with a KAPA SYBR FAST qPCR Kit (NIPPON Genetics, Tokyo, Japan) using a StepOnePlus system (Applied Biosystems, Foster City, CA, USA). Glyceraldehyde 3-phosphate dehydrogenase (GAPDH) was used as internal control. The primer sequences are summarized in Table I.

Statistical analysis. Continuous variables are expressed as mean±standard deviation. Differences among the three groups were analyzed using one-way analysis of variance, and the differences between the two groups were compared using Student's *t*-test. *p*-Values <0.05 were considered statistically significant. All statistical analyses were performed using SAS software (JMP 14.2.0; SAS Institute Inc., Cary, NC, USA).

Results

Comparison of SOS severity among high-dose MCT, low-dose MCT, and control groups. In the high-dose MCT group, macroscopic examination at 48 h after MCT administration showed that the color of the liver's surface had turned dark red. These findings were less pronounced in the low-dose MCT group and control groups (Figure 2A-C). Microscopically, the liver tissue of the rats in the high-dose MCT group displayed severe sinusoidal hemorrhage, sinusoidal dilatation, coagulative necrosis of hepatocytes, and endothelial damage in the central vein. Liver sections from the low-dose MCT group showed less sinusoidal hemorrhage and dilatation compared to those from high-dose MCT group (Figure 2D-I).

To assess the effect of MCT on inusoidal endothelial cells, RECA-1 immunohistochemistry was performed. Areas positive with RECA-1 were larger in the low-dose MCT group than in the high-dose MCT group but smaller than those in the control group (Figure 2J-L).

Regarding serum biochemistry evaluations at 48 h after MCT administration, AST and ALT levels in the low-dose MCT group were significantly lower than those in the high-dose MCT group but were significantly higher than those in the control group. Furthermore, the albumin level in the low-dose MCT group was markedly reduced compared to that in the control group but was higher than that in the high-dose MCT group (Table II).

Accordingly, the high-dose MCT group did not mimic the human SOS induced by oxaliplatin owing to severe hepatotoxicity. Therefore, we defined the low-dose MCT group (70 mg/kg) as the mild SOS group for comparison with the control group in the following experiments.

Comparison of tumor progression between the MCT-induced mild SOS model and control model in the splenic RCN-H4 injection liver metastases model. Twenty-one days after splenic RCN-H4 injection, macroscopic findings showed multiple tumors over the whole liver lobe (Figure 3B), and microscopic findings showed multiple round tumors with internal necrosis in the mild SOS group (Figure 3D and F), compared to the few small tumors scattered in the control group (Figure 3A, C and E). The number of tumors in the mild SOS group (332±213) was significantly higher than that in the control group (16±5) (p=0.029) (Figure 3G).

Comparison of tumor progression between the MCT-induced mild SOS model and control model in the hepatic RCN-H4

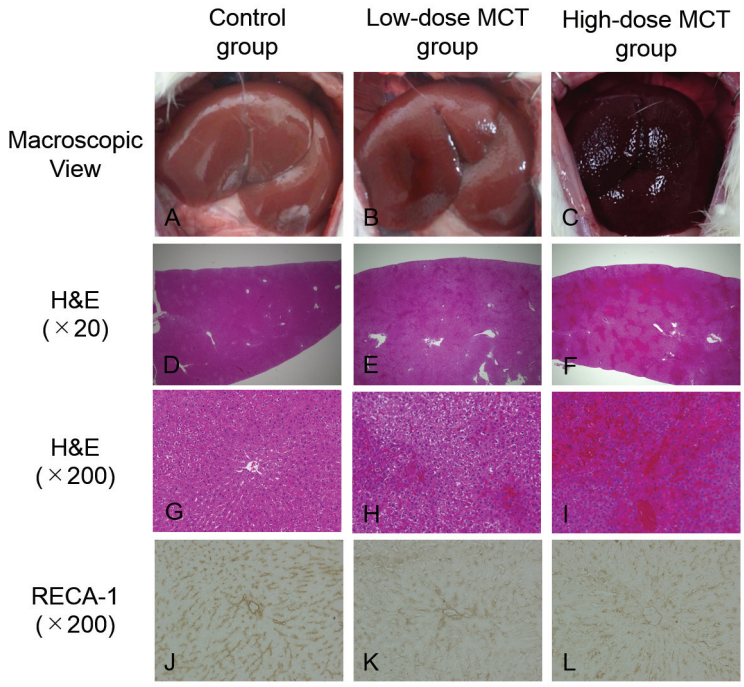

Figure 2. *Effect of monocrotaline (MCT) on liver among high-dose MCT, low-dose MCT, and control groups. Representative macroscopic views of the liver in the control (A), low-dose MCT (B), and high-dose MCT groups (C). H&E staining (×20, ×200) in the control (D and G), low-dose MCT (E and H), and high-dose MCT SOS groups (F and I). Immunohistochemistry of RECA-1 (×200) in the control (J), low-dose MCT (K), and high-dose MCT groups (L).*

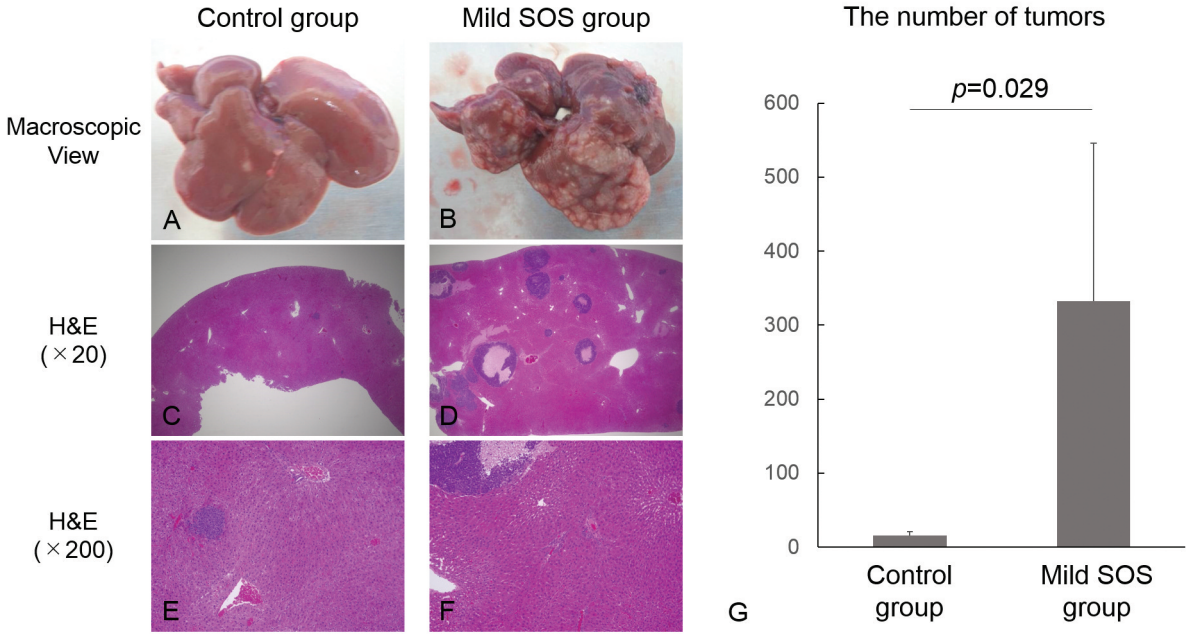

Figure 3. *Assessment of tumor progression in the splenic RCN-H4 injection model. Representative macroscopic views of the liver in the control (A) and mild sinusoidal obstruction syndrome (SOS) groups (B) 21 days after splenic RCN-H4 injection. H&E staining (×20, ×200) in the control (C and E) and mild SOS groups (D and F). The number of tumors in the control and mild SOS groups (G).*

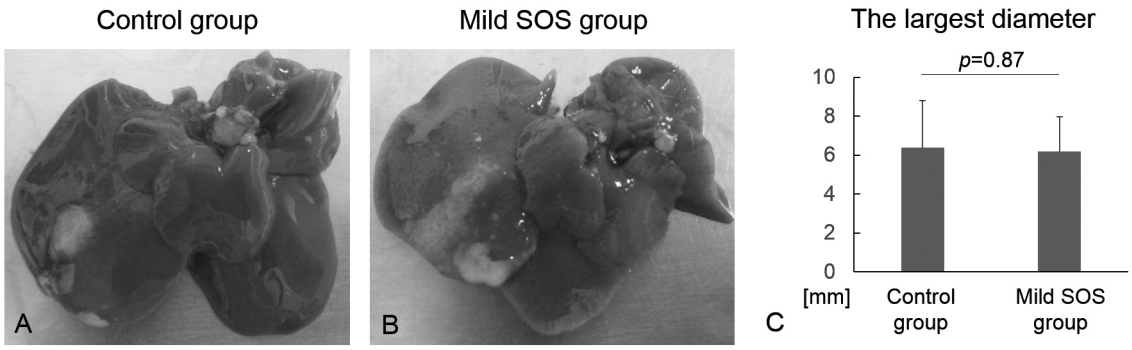

Figure 4. *Assessment of tumor progression in the hepatic RCN-H4 injection model. Representative macroscopic views of the liver in the control (A) and mild sinusoidal obstruction syndrome (SOS) groups (B) 14 days after hepatic RCN-H4 injection. The largest diameter of the locally formed tumor in the control and mild SOS groups (C).*

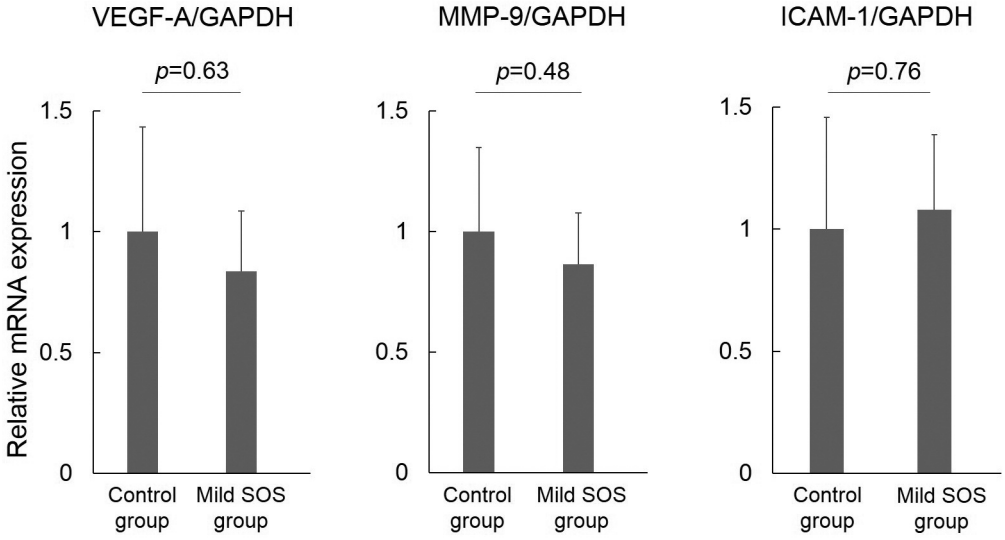

Figure 5. *mRNA expression of genes (VEGF-A, MMP-9 and ICAM-1) 48 h after monocrotaline or vehicle administration between the control group and mild sinusoidal obstruction syndrome (SOS) group.*

Table II. *Serum biochemistry at 48 h after MCT or vehicle administration.*

Variables	Normal range	Control group	Low-dose MCT group	High-dose MCT group	*p*-Value
AST (IU/l)	87-114	77.5±12.7	122.3±8.5	3,861.8±2,625.4	0.0093*#
ALT (IU/l)	28-40	56.8±18.6	100.0±17.8	3,210.0±1,832.3	0.0032*#
Alb (g/dl)	3.3-4.6	3.93±0.13	3.70±0.14	3.45±0.10	0.0014*#

MCT, Monocrotaline; AST, aspartate aminotransferase; ALT, alanine aminotransferase; Alb, albumin. Data are expressed as mean±SD. n=4 in each group. *Significant difference between the control and low-dose MCT groups. #Significant difference between the low- and high-dose MCT groups.

injection liver metastases model. Fourteen days after hepatic RCN-H4 injection, macroscopic findings showed a solitary tumor in the left lateral lobe of the liver in both groups (Figure 4A and B). The largest diameter of the solitary tumor in the mild SOS group (6.2±1.8 mm) was similar to that in the control group (6.4±2.4 mm) (p=0.87) (Figure 4C).

Comparison of hepatic mRNA expression of genes 48 h after MCT or vehicle administration between the MCT-induced mild SOS and control groups. The hepatic expression levels of VEGF-A, MMP-9, and ICAM-1 are shown in Figure 5. There were no significant between-group differences.

Discussion

Our study demonstrated that the low-dose MCT group (70 mg/kg) showed better characteristics as a mimic rat model of human oxaliplatin-induced SOS than the high-dose MCT (90 mg/kg) group and defined a low-dose MCT group as the mild SOS group. Mild SOS promoted CRLM development only in the splenic injection liver metastases model.

The promotion of CRLM has been evaluated by hepatic ischemia and reperfusion injury (21), nonalcoholic steatosis (22) and chronic alcohol consumption (23) rodent models, and these liver injuries affect CRLM tumor growth. The promotion of lung metastases in a pulmonary hypertension model by subcutaneous administration of 60 mg/kg MCT was assessed, and lung injury induced by MCT resulted in lung tumor growth (24). In humans, SOS after neoadjuvant chemotherapy with oxaliplatin was associated with decreased long-term survival in CRLM, but its mechanism remains unclear (9). Our present study provided similar results in a rat SOS model as a clinical outcome.

In previous studies, severe and acute liver injury with AST and ALT levels greater than 1,000 IU/l have been commonly used in MCT-induced (90 mg/kg or more) SOS rat models (12, 25). However, the presence of SOS was not associated with elevated liver transaminases in a human clinical study (9). To further mimic the preoperative chemotherapy treatment of CRLM in humans, we created a mild SOS model with AST and ALT around 100 IU/l and used it in experiments.

According to the experimental results, there was a significant difference between the control and mild SOS groups when cancer cells were administered in the spleen, but no difference was observed between the two groups when cancer cells were administered in the liver. Thus, clinical data reported by Tamandl *et al*. (9) were corroborated only in the splenic injection model. Regarding the involvement of endothelial damage, which they also speculated as a mechanism by which SOS affects long-term prognosis (9), our results suggest that the process of cancer cell entry into the liver *via* circulation rather than the background liver damage associated with SOS may be the cause of tumor growth.

There are several possible mechanisms for the effects of background liver damage on liver metastases. First, it has been reported that bevacizumab, a monoclonal antibody that inhibits VEGF-A, suppresses human SOS (26), suggesting that the expression of VEGF-A may be involved in tumor progression. Secondly, MMP-9 inhibition has been reported to inhibit MCT-induced SOS in rats (25), which indicates that MMP-9 may also be involved in tumor growth. Third, the process by which cancer cells bind to ICAM-1 in sinusoidal endothelial cells (SECs) (27) may lead to accelerated liver metastases by SOS-induced hepatic damage. However, these mechanisms were considered unlikely since the analysis of background liver mRNA showed no significant differences between the mild SOS and control groups with respect to VEGF-A, MMP-9, and ICAM-1. If the entry of cancer cells into the liver is accelerated by SOS, it is possible that endothelial cell damage, a hallmark of SOS, may be a factor. It is reported that the liver exhibited high expression of lectin molecules and liver sinusoidal endothelial cell lectin, which is a liver-specific adhesion molecule, plays an important role in CRLM (28, 29). Analysis from that perspective may be useful for future study.

This study had several limitations. First, the precise mechanism by which SOS affects CRLM development has not yet been clarified. The mechanism of SOS in the MCT-induced rat model was described as follows (10, 25, 30). The gap created by detached SECs from the sinusoidal walls, which are typical features of SOS, may make it easier for cancer cells to invade hepatic parenchymal cells. It is also possible that the damaged sinusoidal wall endothelial cells are more likely to adhere to cancer cells. In elucidating these processes, visualization of a single cancer cell tagged with a fluorescent dye may be useful to track the distribution and movement of cancer cells during the pre-tumor stage in future studies. For this purpose, it is necessary to first evaluate the appropriate timing of cancer cell attachment to the sinusoidal endothelium after splenic cancer cell injection. Second, the solution to this phenomenon has not been explored. It is worth examining whether the prevention of SOS, which we have already reported (12-16), can reduce the progression of these tumors. If they affect not only postoperative morbidity but also long-term outcomes, the significance of their clinical application could be further strengthened. Third, this MCT-induced mild SOS rat model may be still somewhat different from oxaliplatin-induced SOS in humans. In clinical practice, oxaliplatin is commonly used in combination with fluoropyrimidines including oral S-1 and capecitabine, which are converted to 5-fluorouracil in the liver. Recently, it has been reported that concomitant use of S-1 increases the frequency and severity of SOS (31), and the mechanism regarding the effect of concomitant fluoropyrimidines may need to be clarified.

In conclusion, mild SOS induced by MCT promotes CRLM development in splenic RCN-H4 injection liver metastases rat model. In contrast, mild SOS does not promote CRLM development in hepatic RCN-H4 injection liver metastases rat model. The process of cancer cell entry into the liver *via* portal

circulation may be associated with tumor growth. Further studies are needed to clarify these mechanisms.

Conflicts of Interest

None to be declared.

Authors' Contributions

H.N., M.O., and E.H. designed the experiments. H.N., R.T., K.Y., Y.K., and M.S. were involved in the acquisition of the data. S.S., K.I., and K.T. provided technical support and conceptual advice. H.N. and M.O. were involved in writing the manuscript. All authors were involved in the final manuscript editing and approval.

Acknowledgements

This study was supported in part by JSPS KAKENHI Grant Number 19K24009.

References

1 Manfredi S, Lepage C, Hatem C, Coatmeur O, Faivre J and Bouvier AM: Epidemiology and management of liver metastases from colorectal cancer. Ann Surg *244(2)*: 254-259, 2006. PMID: 16858188. DOI: 10.1097/01.sla.0000217629.94941.cf

2 Adam R, De Gramont A, Figueras J, Guthrie A, Kokudo N, Kunstlinger F, Loyer E, Poston G, Rougier P, Rubbia-Brandt L, Sobrero A, Tabernero J, Teh C, Van Cutsem E and Jean-Nicolas Vauthey of the EGOSLIM (Expert Group on OncoSurgery management of LIver Metastases) group: The oncosurgery approach to managing liver metastases from colorectal cancer: A multidisciplinary international consensus. Oncologist *17(10)*: 1225-1239, 2012. PMID: 22962059. DOI: 10.1634/theoncologist.2012-0121

3 Bismuth H, Adam R, Lévi F, Farabos C, Waechter F, Castaing D, Majno P and Engerran L: Resection of nonresectable liver metastases from colorectal cancer after neoadjuvant chemotherapy. Ann Surg *224(4)*: 509-520; discussion 520-2, 1996. PMID: 8857855. DOI: 10.1097/00000658-199610000-00009

4 Adam R, Laurent A, Azoulay D, Castaing D and Bismuth H: Two-stage hepatectomy: A planned strategy to treat irresectable liver tumors. Ann Surg *232(6)*: 777-785, 2000. PMID: 11088072. DOI: 10.1097/00000658-200012000-00006

5 Okuno M, Hatano E, Kasai Y, Nishio T, Seo S, Taura K, Yasuchika K, Nitta T, Mori A, Okajima H, Kaido T, Hasegawa S, Matsumoto S, Sakai Y and Uemoto S: Feasibility of the liver-first approach for patients with initially unresectable and not optimally resectable synchronous colorectal liver metastases. Surg Today *46(6)*: 721-728, 2016. PMID: 26315324. DOI: 10.1007/s00595-015-1242-z

6 Rubbia-Brandt L, Audard V, Sartoretti P, Roth AD, Brezault C, Le Charpentier M, Dousset B, Morel P, Soubrane O, Chaussade S, Mentha G and Terris B: Severe hepatic sinusoidal obstruction associated with oxaliplatin-based chemotherapy in patients with metastatic colorectal cancer. Ann Oncol *15(3)*: 460-466, 2004. PMID: 14998849. DOI: 10.1093/annonc/mdh095

7 Nakano H, Oussoultzoglou E, Rosso E, Casnedi S, Chenard-Neu MP, Dufour P, Bachellier P and Jaeck D: Sinusoidal injury increases morbidity after major hepatectomy in patients with colorectal liver metastases receiving preoperative chemotherapy. Ann Surg *247(1)*: 118-124, 2008. PMID: 18156931. DOI: 10.1097/SLA.0b013e31815774de

8 Rubbia-Brandt L: Sinusoidal obstruction syndrome. Clin Liver Dis *14(4)*: 651-668, 2010. PMID: 21055688. DOI: 10.1016/j.cld.2010.07.009

9 Tamandl D, Klinger M, Eipeldauer S, Herberger B, Kaczirek K, Gruenberger B and Gruenberger T: Sinusoidal obstruction syndrome impairs long-term outcome of colorectal liver metastases treated with resection after neoadjuvant chemotherapy. Ann Surg Oncol *18(2)*: 421-430, 2011. PMID: 20844968. DOI: 10.1245/s10434-010-1317-4

10 DeLeve LD, McCuskey RS, Wang X, Hu L, McCuskey MK, Epstein RB and Kanel GC: Characterization of a reproducible rat model of hepatic veno-occlusive disease. Hepatology *29(6)*: 1779-1791, 1999. PMID: 10347121. DOI: 10.1002/hep.510290615

11 Kumar A, Palek R and Liska V: A critical analysis of experimental animal models of sinusoidal obstruction syndrome. J Clin Exp Hepatol *9(3)*: 345-353, 2019. PMID: 31360027. DOI: 10.1016/j.jceh.2018.07.002

12 Narita M, Hatano E, Ikai I, Miyagawa-Hayashino A, Yanagida A, Nagata H, Asechi H, Taura K and Uemoto S: A phosphodiesterase III inhibitor protects rat liver from sinusoidal obstruction syndrome through heme oxygenase-1 induction. Ann Surg *249(5)*: 806-813, 2009. PMID: 19387321. DOI: 10.1097/SLA.0b013e3181a38ed5

13 Narita M, Hatano E, Tamaki N, Yamanaka K, Yanagida A, Nagata H, Asechi H, Takada Y, Ikai I and Uemoto S: Dai-kenchu-to attenuates rat sinusoidal obstruction syndrome by inhibiting the accumulation of neutrophils in the liver. J Gastroenterol Hepatol *24(6)*: 1051-1057, 2009. PMID: 19638085. DOI: 10.1111/j.1440-1746.2009.05795.x

14 Nakamura K, Hatano E, Narita M, Miyagawa-Hayashino A, Koyama Y, Nagata H, Iwaisako K, Taura K and Uemoto S: Sorafenib attenuates monocrotaline-induced sinusoidal obstruction syndrome in rats through suppression of JNK and MMP-9. J Hepatol *57(5)*: 1037-1043, 2012. PMID: 22796153. DOI: 10.1016/j.jhep.2012.07.004

15 Nakamura K, Hatano E, Miyagawa-Hayashino A, Okuno M, Koyama Y, Narita M, Seo S, Taura K and Uemoto S: Soluble thrombomodulin attenuates sinusoidal obstruction syndrome in rat through suppression of high mobility group box 1. Liver Int *34(10)*: 1473-1487, 2014. PMID: 24498917. DOI: 10.1111/liv.12420

16 Okuno M, Hatano E, Nakamura K, Miyagawa-Hayashino A, Kasai Y, Nishio T, Seo S, Taura K and Uemoto S: Regorafenib suppresses sinusoidal obstruction syndrome in rats. J Surg Res *193(2)*: 693-703, 2015. PMID: 25266603. DOI: 10.1016/j.jss.2014.08.052

17 Prié S, Stewart DJ and Dupuis J: EndothelinA receptor blockade improves nitric oxide-mediated vasodilation in monocrotaline-induced pulmonary hypertension. Circulation *97(21)*: 2169-2174, 1998. PMID: 9626178. DOI: 10.1161/01.cir.97.21.2169

18 Inoue Y, Kashima Y, Aizawa K and Hatakeyama K: A new rat colon cancer cell line metastasizes spontaneously: Biologic characteristics and chemotherapeutic response. Jpn J Cancer Res *82(1)*: 90-97, 1991. PMID: 1900274. DOI: 10.1111/j.1349-7006.1991.tb01751.x

19 Okuno K, Hirai N, Lee YS, Kawai I, Shigeoka H and Yasutomi M: Involvement of liver-associated immunity in hepatic metastasis formation. J Surg Res *75(2)*: 148-152, 1998. PMID: 9655087. DOI: 10.1006/jsre.1998.5272

20 Brand MI, Casillas S, Dietz DW, Milsom JW and Vladisavljevic A: Development of a reliable colorectal cancer liver metastasis model. J Surg Res *63(2)*: 425-432, 1996. PMID: 8661237. DOI: 10.1006/jsre.1996.0287

21 Doi K, Horiuchi T, Uchinami M, Tabo T, Kimura N, Yokomachi J, Yoshida M and Tanaka K: Hepatic ischemia-reperfusion promotes liver metastasis of colon cancer. J Surg Res *105(2)*: 243-247, 2002. PMID: 12121713. DOI: 10.1006/jsre.2002.6356

22 VanSaun MN, Lee IK, Washington MK, Matrisian L and Gorden DL: High fat diet induced hepatic steatosis establishes a permissive microenvironment for colorectal metastases and promotes primary dysplasia in a murine model. Am J Pathol *175(1)*: 355-364, 2009. PMID: 19541928. DOI: 10.2353/ajpath.2009.080703

23 Im HJ, Kim HG, Lee JS, Kim HS, Cho JH, Jo IJ, Park SJ and Son CG: A preclinical model of chronic alcohol consumption reveals increased metastatic seeding of colon cancer cells in the liver. Cancer Res *76(7)*: 1698-1704, 2016. PMID: 26857263. DOI: 10.1158/0008-5472.CAN-15-2114

24 Vincic L, Orr FW, Warner DJ, Suyama KL and Kay JM: Enhanced cancer metastasis after monocrotaline-induced lung injury. Toxicol Appl Pharmacol *100(2)*: 259-270, 1989. PMID: 2506673. DOI: 10.1016/0041-008x(89)90312-8

25 Deleve LD, Wang X, Tsai J, Kanel G, Strasberg S and Tokes ZA: Sinusoidal obstruction syndrome (veno-occlusive disease) in the rat is prevented by matrix metalloproteinase inhibition. Gastroenterology *125(3)*: 882-890, 2003. PMID: 12949732. DOI: 10.1016/s0016-5085(03)01056-4

26 Ribero D, Wang H, Donadon M, Zorzi D, Thomas MB, Eng C, Chang DZ, Curley SA, Abdalla EK, Ellis LM and Vauthey JN: Bevacizumab improves pathologic response and protects against hepatic injury in patients treated with oxaliplatin-based chemotherapy for colorectal liver metastases. Cancer *110(12)*: 2761-2767, 2007. PMID: 17960603. DOI: 10.1002/cncr.23099

27 Van den Eynden GG, Majeed AW, Illemann M, Vermeulen PB, Bird NC, Høyer-Hansen G, Eefsen RL, Reynolds AR and Brodt P: The multifaceted role of the microenvironment in liver metastasis: biology and clinical implications. Cancer Res *73(7)*: 2031-2043, 2013. PMID: 23536564. DOI: 10.1158/0008-5472.CAN-12-3931

28 Martens JH, Kzhyshkowska J, Falkowski-Hansen M, Schledzewski K, Gratchev A, Mansmann U, Schmuttermaier C, Dippel E, Koenen W, Riedel F, Sankala M, Tryggvason K, Kobzik L, Moldenhauer G, Arnold B and Goerdt S: Differential expression of a gene signature for scavenger/lectin receptors by endothelial cells and macrophages in human lymph node sinuses, the primary sites of regional metastasis. J Pathol *208(4)*: 574-589, 2006. PMID: 16440291. DOI: 10.1002/path.1921

29 Zuo Y, Ren S, Wang M, Liu B, Yang J, Kuai X, Lin C, Zhao D, Tang L and He F: Novel roles of liver sinusoidal endothelial cell lectin in colon carcinoma cell adhesion, migration and *in vivo* metastasis to the liver. Gut *62(8)*: 1169-1178, 2013. PMID: 22637699. DOI: 10.1136/gutjnl-2011-300593

30 DeLeve LD, Ito Y, Bethea NW, McCuskey MK, Wang X and McCuskey RS: Embolization by sinusoidal lining cells obstructs the microcirculation in rat sinusoidal obstruction syndrome. Am J Physiol Gastrointest Liver Physiol *284(6)*: G1045-G1052, 2003. PMID: 12584111. DOI: 10.1152/ajpgi.00526.2002

31 Kim EJ, Kim M, Seo S, Kim MJ, Kim MJ and Park SR: Comparison of sinusoidal obstruction syndrome in gastric cancer patients receiving S-1/oxaliplatin *versus* capecitabine/oxaliplatin. Anticancer Res *41(1)*: 391-402, 2021. PMID: 33419836. DOI: 10.21873/anticanres.14788

Received February 1, 2021
Revised March 13, 2021
Accepted March 16, 2021